https://dx.doi.org/10.1016/j.renene.2022.02.127

Manganese Glycerolate Catalyzed Simultaneous Esterification and Transesterification: The Kinetic and Mechanistic Study, and Application in Biodiesel and Bio-Lubricants Synthesis

Pak-Chung Lau, Tsz-Lung Kwong * and Ka-Fu Yung *

Department of Applied Biology and Chemical Technology, The Hong Kong Polytechnic University, Hung Hom, Kowloon, Hong Kong

*** Corresponding author:**

tlsamuel.kwong@polyu.edu.hk (T.-L. Kwong); bckfyung@polyu.edu.hk (K.-F. Yung)

Manganese Glycerolate Catalyzed Simultaneous Esterification and Transesterification: The Kinetic and Mechanistic Study, and Application in Biodiesel and Bio-Lubricants Synthesis

Abstract

Several characterizations (BET, BJH, XPS, and elemental analysis) were employed further to examine the manganese glycerolate. The elemental analysis proved that the ratio of manganese-to-glycerol is 3:4. The MnGly catalyst is formed as a mixed-valence compound in an Mn^{2+} to Mn^{3+} ratio of 1:2 that aligned the results of the surface ratio of Mn^{2+} to Mn^{3+} from XPS analysis. This compound provides a total of eight positive charges to compensate for the eight negative charges generated from the hydroxyl group (-OH) in four glycerol ligands. The activation energy (112.7 kJ mol^{-1}) suggests that the reaction undergoes surface-mediated catalysis. The XPS analysis and kinetic study prove the co-existence of divalent and trivalent manganese in MnGly catalyst, demonstrating a flexible coordination geometry between tetrahedral and octahedral. It facilitates the coordination of two methanol to Mn^{2+} center with an octahedral geometry as the first step of the mechanism for biodiesel synthesis. The yield could achieve more than 99% in 1.5 hours under the optimized reaction conditions. The ANOVA revealed that reaction temperature is the most significant factor affecting the production of FAME, with a contribution of 82.84%. This catalytic system also demonstrated high compatibility with higher alcohols for exploring bio-lubricants.

Keywords

Kinetic study; mechanistic study; biodiesel; bio-lubricants; manganese glycerolate; simultaneous esterification and transesterification

Nomenclature

FAME	Fatty acid methyl ester
FFA	Free fatty acid
E_a	Activation energy
BET	Brunauer-Emmett-Teller
BJH	Barrett-Joyner- Halenda
XPS	X-ray photoelectron spectroscopy
^{1}H-NMR	^{1}H nuclear magnetic resonance
TPD	Temperature programmable desorption
TCD	Thermo-conductivity detector
ICO-OES	Inductively-coupled plasma optical emission spectroscopy
ANOVA	Analysis of variance
OA	Orthogonal array

1. Introduction

The rapid population growth and economic development in modern society have resulted in high energy consumption. The depletion of limited fossil fuel reserves and the generation of greenhouse gases upon burning have prompted researchers to find an alternative renewable fuel [1]. To sustain the high energy demand and reduce environmental pollution, finding alternative renewable energy sources has become necessary in the future.

Biodiesel is a mixture of fatty acid methyl esters (FAMEs), which can replace petroleum-based fuels directly due to their similarity of physical and chemical properties [2]. Biodiesel is considered one of the alternative renewable fuels due to its unlimited reserve, carbon neutrality, biodegradability, and non-toxicity with low sulfur content, which can be made from different vegetable oils (edible oil or non-edible oil) or animal fats as feedstock [3-5]. However, the cost of feedstock accounts for 70 – 80 % of biodiesel's total production cost, which is the main barrier to commercialization in the market [6, 7]. The application of low-grade non-refined feedstock containing high free fatty acid (FFA) contaminants on biodiesel synthesis is economically beneficial by reducing the cost of raw material [8]. In order to deal with the high FFA containing low-grade non-refined feedstock, searching for a promising catalyst that supports simultaneous esterification of FFA and transesterification of triglycerides is of great interest to the field of renewable liquid fuel technology.

Homogeneous catalysis by applying strong acid and alkali is the traditional way to give a high yield. However, the presence of FFA in non-refined feedstock causes soap formation in base-catalyzed reactions [9]. Although homogeneous acid catalysts can simultaneously catalyze esterification and transesterification, their slow reaction kinetics, corrosiveness to reaction equipment, and the generation of a massive amount of wastewater in diluting the catalyst are disadvantageous. The limitation of separation and recovery of catalyst is another issue that hinders the development of homogeneous catalysis towards biodiesel synthesis [10].

The use of heterogeneous catalysts has resolved the above drawbacks [11]. However, the presence of water and FFA in low-grade reagents often induces saponification and causes the deactivation of heterogeneous base catalysts unless some pre-treatment steps are performed [12]. Hence, a growing trend in investigating a heterogeneous catalyst that exhibits remarkable stability upon regeneration and high tolerance to FFA and water in the feedstock.

The application of different metal carboxylates as a heterogeneous catalyst towards biodiesel synthesis has been reported. A series of layered zinc, copper (II), manganese (II), and nickel (II) carboxylates were synthesized that showed significant conversion in 2 hours [13, 14]. However, the catalytic instability due to leaching, reconstruction, and transformation of those carboxylates after the reaction was observed. Reinoso *et al.* [15] reported that the application of zinc glycerolates (ZnGly) as an effective catalyst in biodiesel synthesis exhibited long life reusability, robustness, and moderate tolerance towards FFA and water.

Recently, we studied the reaction mechanism of simultaneous esterification and transesterification using zinc oxide (ZnO) nanostar as a model catalyst and discovered that zinc oleate (ZnOl) is involved as an intermediate and transformed to ZnGly and finally re-deposit on the ZnO as ZnGly/ZnO co-catalyst [16]. Based on the above findings, we developed different transition metal glycerolates and found that manganese glycerolates (MnGly) gave the highest catalytic activity towards transesterification reaction [17].

In this present study, manganese glycerolate (MnGly) catalyst was further examined using several surface characterizations such as BET, BJH, XPS, and elemental analysis. A detailed understanding of the chemistry and the mechanism involved in MnGly catalyzed biodiesel synthesis was thoroughly discussed. The reaction kinetics of this catalytic system was also investigated, and its activation energy (E_a) was also determined. A study of the effect of reaction temperature, feedstock-to-methanol molar ratio, catalyst loading, and oleic acid loading was investigated through Taguchi analysis. Optimizing reaction conditions is vital in synthesizing biodiesel to maximize the product yield and minimize the production cost. The conventional stepwise approach dealing with a full-scale optimization is relatively time-consuming and inefficient [18]. Taguchi approach is an effective way of optimization that uses orthogonal array experimental design to organize all the factors and levels to be optimized [19-21]. The selection of desirable levels from each factor and the significance of each factor would be determined by a statistical model of analysis of variance (ANOVA). This would help to evaluate the possibility of applying the as-synthesized MnGly catalyst in the bio-lubricants synthesis using higher alcohol sources and microwave irradiation as a heating source.

2. Materials and methods

2.1. Materials

Refined food-grade canola oil was purchased from a local store in Hong Kong. Manganese (II) acetate tetrahydrate ($(CH_3COO)_2Mn{\cdot}4H_2O$, 97 %) was obtained from Fraco Chemical Supplies. Glycerol ($C_3H_8O_3$) was separated and obtained in biodiesel synthesis. Methanol (CH_3OH, 99.8 %), ethanol (C_2H_5OH, 99.0 %) and 1-butanol (C_4H_9OH, 99.0 %) of reagent grade were supplied by ACS while 1-propanol (C_3H_7OH, >99 %), was purchased from Acros. 1-pentanol ($C_5H_{11}OH$, 99.0 %), 1-hexanol ($C_6H_{13}OH$, 99.0 %), and 1-heptanol ($C_7H_{15}OH$, 99.0 %) of laboratory reagent grade were provided by BDH Chemical Ltd. Oleic acid ($C_{18}H_{34}O_2$, 99.9 %) was purchased as laboratory reagent grade from Fisher Chemical. Methyl yellow, neutral red, bromothymol blue, and phenolphthalein were supplied from Sigma Aldrich.

2.2. Synthesis and characterization of catalyst

Manganese glycerolates (MnGly) nano-plate catalyst was synthesized by microwave-assisted hydrothermal synthesis reported in our previous study [17].

Nitrogen adsorption-desorption isotherm of the catalyst was measured on Micrometritics ASAP2020 Automatic Micropore and Chemisorption Physisorption Analyzer. The catalyst was outgassed before the analysis at 350 °C for 10 hours initiated with a rate of 10 °C min^{-1}. The analysis was held under vacuum throughout the entire analysis using N_2 at 77 K with a P/P_0 range of 0.01 to 0.995. The surface area and pore size distribution were determined based on Brunauer-Emmett-Teller (BET) and Barrett-Joyner- Halenda (BJH) theories.

Hammett indicator analysis was used to elucidate the surface basicity of MnGly catalyst in which methyl yellow ($H\_$ = 3.3), neutral red ($H\_$ = 6.8), bromothymol blue ($H\_$ = 7.2), and phenolphthalein ($H\_$ = 9.7) were used as Hammett indicators. MnGly catalyst (5 mg) was immersed in methanolic Hammett indicator solution (1 mL, 50 μM).

The elemental composition of C and H of the MnGly catalyst was analyzed by Elementar Vario MICRO Select elemental combustion analyzer. The sample catalyst (<5 mg) was combusted under high temperatures that led to the formation of H_2O and CO_2. The resultant analyte gases with helium carrier

gas would then pass through the temperature programmable desorption (TPD) column for sequential separation and finally a thermo-conductivity detector (TCD) for quantitative detection. Meanwhile, the elemental composition of manganese (Mn) in MnGly was deduced by inductively-coupled plasma optical emission spectroscopy (ICP-OES) on Agilent Technologies 700 Series ICP-OES. The sample solution was prepared by digesting the catalyst (25 mg) under heating at 60 °C into concentrated hydrochloric acid (3 mL) and concentrated nitric acid (1 mL) for 2 hours, followed by dilution with nitric acid (1%).

The oxidation state of each catalyst element was characterized by Axis Ultra DLD X-ray photoelectron spectroscopy (XPS) using AlKα radiation of 1486.6 eV with an electron take-off angle at 90^{o} in which the pressure in the sample chamber was kept at 10^{-8} Torr.

2.3. The catalytic reaction of simultaneous esterification and transesterification and biodiesel yield determination

The catalytic reactions for biodiesel synthesis were conducted in a pressurized reactor containing MnGly catalyst, alcohols, and feedstock sample (0.46 g) with different ratios specified in the results and discussion. The reaction was heated with a constant stirring at 750 rpm at the corresponding reaction temperature and time. The synthesized biodiesel layer was separated from the catalyst by centrifugation.

For the kinetic study, the catalytic reactions were performed in a pressurized reactor containing the MnGly catalyst (6 wt.%), feedstock sample, and methanol in a ratio of 1:40. The catalytic reaction was tested with a constant stirring at 750 rpm at the different reaction temperatures of 130 °C, 140 °C, and 150 °C for 30 minutes. The sample was collected to determine the yield at 10 min, 20 min, and 30 min.

The biodiesel yield was analyzed by ^{1}H nuclear magnetic resonance (^{1}H-NMR) spectroscopy on Bruker 400 MHz spectrometer using $CDCl_3$ as the solvent. The FAME yield was calculated based on the integral area of peak signal of alkoxy proton (-OCH_3) on FAME at around 3.6 - 4 ppm and signal of the α-methylene proton (α-CH_2) on triglyceride and fatty acid alkyl ester at 2.3 ppm. The calculation of FAME yield is shown in Equation 1 [22].

$$\text{Yield}(\%) = \frac{A_{\text{-OCH}_3}/3}{A_{\alpha\text{-CH}_2}/2} \times 100\% \quad (1)$$

164

165 *2.4. Determination of reaction kinetics*

166 In the case of heterogeneous catalysis, the overall rate equation would become more complicated
167 due to adsorption and desorption of catalysts and diffusion. Therefore, a more sophisticated kinetics
168 model involving the order of reaction for triglyceride and alcohol should be utilized [23]. The catalytic
169 reaction rate is based on the decrease in the amount of feedstock. The reaction order with respect to
170 the triglycerides and methanol for a simple transesterification can be determined by the following
171 equation,

$$-\frac{dC_{TG}}{dt} = kC_{TG}^{\alpha}C_{Me}^{\beta} \quad (2)$$

172 where $-\frac{dC_{TG}}{dt}$ is the rate of triglyceride consumption per unit time *t*; *k* is the rate constant; C_{TG} and C_{Me}
173 are the concentrations of triglyceride and methanol respectively after time *t*; α and β are the order of
174 reaction with respect to triglyceride and methanol respectively.

175 The change of concentration of the reactants are presented as follows,

$$C_{TG} = C_{TG0}(1\text{-}X) \quad (3)$$

$$C_{Me} = C_{TG0}(\eta\text{-}3X) \quad (4)$$

$$\eta = \frac{C_{Me0}}{C_{TG0}} \quad (5)$$

$$\frac{dX}{dt} = kC_{TG0}^{(\alpha+\beta-1)}(1\text{-}X)^{\alpha}(\eta\text{-}3X)^{\beta} \quad (6)$$

176 where C_{TG0} and C_{Me0} are the initial concentration of triglyceride and methanol, X is the conversion, and
177 η is the ratio of C_{Me0}-to-C_{TG0}.

178 Based on Equation 6, three scenarios of varying reaction order with respect to triglyceride and
179 methanol were set up, including (α = 0, β = 0), (α = 1, β = 0), and (α = 2, β = 0). The detailed on the
180 definite integrals of the substituted rate equations have been shown in Table S1 in Supplementary

materials. The exact reaction order would be selected from the scenario with the highest correlation coefficients (R^2) and the rate constant (k) would be determined from the slope of the straight line.

The activation energy (E_a) of the catalytic reaction was calculated based on the rate constants obtained from different reaction temperatures [24]. It can be deduced from the slope of ln k against 1/T according to the Arrhenius equation as shown from Equations 7 and 8.

$$k = Ae^{-E_a/RT} \quad (7)$$

$$\ln k = \frac{-E_a}{RT} + \ln A \quad (8)$$

where k is the rate constant, R is the universal gas constant (8.314 J mol^{-1} K^{-1}), T is the reaction temperature in Kelvin, and A is the pre-exponential factor.

2.5. Design of experiment for optimization

Refined canola oil was used as the feedstock containing a trace amount of FFA and water, while oleic acid was used as the model of FFA in this investigation. Reaction temperature (factor A), feedstock-to-methanol molar ratio (factor B), catalyst loading (factor C), and oleic acid loading (factor D) are the factors to be optimized through Taguchi analysis and further analyzed by analysis of variance (ANOVA). Each factor is associated with four levels, as shown in Table 1.

Table 1

Factors and levels selected for catalytic reaction conditions optimization.

Level (i)	Factor (j)			
	Reaction temperature A (°C)	**Feedstock-to-methanol molar ratio B**	**Catalyst loading C (wt.%)**	**Oleic acid loading D (wt.%)**
1	120	1:10	2	2.5
2	130	1:20	4	5
3	140	1:30	6	7.5
4	150	1:40	8	10

3. Results and discussion

3.1. Catalyst characterization

The MnGly catalyst was characterized by SEM, XRD, and FTIR analysis and their results have been reported in our previous study [17]. Therefore, the details on the above characterization are not included here.

The textural properties of MnGly catalyst, such as BET surface area, pore diameter, and pore volume, were determined by nitrogen adsorption-desorption analyzer, and the results are depicted in Fig.1a. It is proved that the MnGly catalyst exhibited a type III isotherm which indicates a weak interaction between adsorbate and adsorbent. Therefore, the monolayer coverage or formation information is unclear [25]. A hysteresis loop in P/P_0 ranging from 0.9 to 1.0 is attributed to a type H3 hysteresis loop. The H3 hysteresis loop does not demonstrate any plateau of adsorption isotherm at high relative pressure, revealing that the non-rigid aggregation of plate-like particles gives rise to slit-shaped pores [26]. In addition, the specific surface area of the MnGly catalyst was measured to be 33.7 m^2/g, as determined from the BET method. BJH analysis shows a narrow distribution of pores for MnGly catalyst with the pore volume of 0.05 cm^3/g and pore diameter of 2.94 nm, which indicates the MnGly catalyst is mesoporous (Fig. 1b).

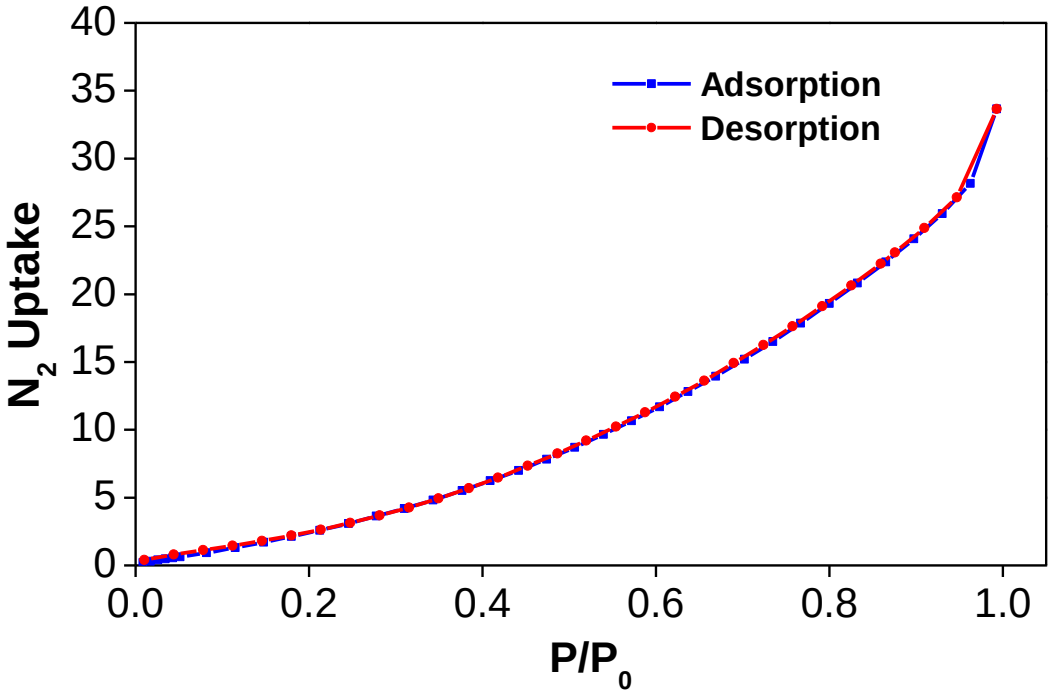

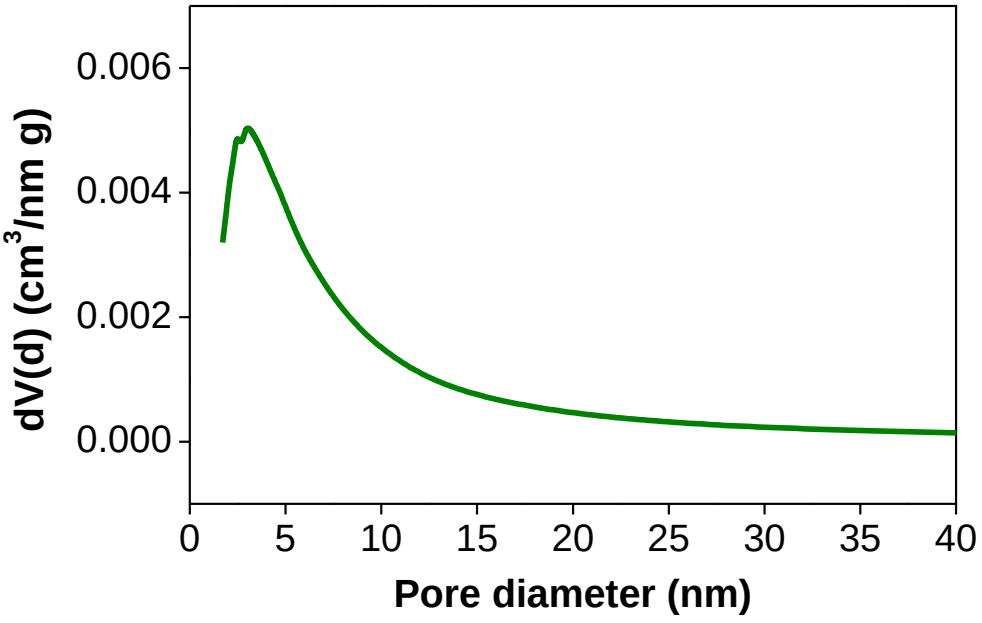

Fig. 1. (**a**) N_2 adsorption-desorption isotherm and (**b**) the corresponding BJH pore size distribution of MnGly catalyst.

From the result of Hammett indicator analysis, the surface basic strength ($H\_$) of MnGly catalyst was found to be in the range of $6.8 < H\_ < 7.2$, which exhibits the amphoteric property on the surface of MnGly catalyst. As a result, MnGly is verified to be a potential heterogeneous catalyst towards

simultaneous esterification and transesterification reaction for biodiesel synthesis as it could exhibit a high tolerance towards FFA without inducing saponification during the catalytic reaction.

The elemental compositions of carbon (C) and hydrogen (H) for MnGly catalyst were determined by elemental combustion analyzer, while that of manganese (Mn) was done by employing ICP-OES. The experimental results and the calculated theoretical ratios based on the proposed empirical chemical formulas are summarized in Table 2. The empirical chemical formula for MnGly catalyst is proposed to be $C_{12}H_{24}O_{12}Mn_3$ as the basic unit in which the ratio of Mn-to-Gly is 3:4. The experimental results are nearly identical to the calculated elemental ratios with only slight deviations. Therefore, it is rational to conclude that the actual empirical formula of MnGly catalyst is most likely analogous to the proposed formula. In general, the MnGly might aggregate through the intermolecular Mn---O interaction from the Lewis basic oxygen atoms on the ligand framework to fulfill the coordination sphere of the Mn metal. The MnGly catalyst maybe existed in the polymeric form with aggregation instead of the monomeric form based on the result of the elemental analysis. It is generally accepted that the monomeric form of MnGly could be associated with the coordination of water molecules to the Mn metal center. In the case of the monomeric structure consisting of three water molecules, the vastly different elemental ratio of C: 24.9%, H: 5.2%, and Mn: 28.5% should be observed. However, it is obvious to notify that the experimental determining elemental composition of MnGly catalyst matches well with the proposed empirical formula of $C_{12}H_{24}O_{12}Mn_3$ in the absence of water. Therefore, it proves the possibility for the formation oligomer or polymer of MnGly in which the ratio of Mn-to-Gly is 3:4. Furthermore, the MnGly catalyst is likely to be formed as a mixed-valence compound in a ratio of divalent (Mn^{2+})-to-trivalent (Mn^{3+}) of 1:2, which provides a total of eight positive charges to compensate the eight negative charges generated from the hydroxyl group (-OH) in glycerol.

Table 2

Elemental composition of C, H, and Mn for MnGly nano-plates catalyst.

Elemental composition	**Found (Calculated)/ %**		
	C	**H**	**Mn**
MnGly	27.2 (27.4)	4.5 (4.6)	32.0 (31.4)

The XPS analysis is a non-destructive and systematic method to determine the existence of elements and their oxidation states. The XPS spectrum of MnGly nano-plates catalyst is depicted in Fig. 2. The symmetrical C 1s peak at 286.4 eV was detected (Fig 2b). The asymmetric O 1s peak at 531.5 eV is further resolved into two peaks at 531.5 eV and 532.3 eV, which are attributed to hydroxyl oxygen from water and oxygen from C-O single bond in glycerol, respectively (Fig 2c). Fig. 2d shows the two peaks at 641.1 eV and 653.8 eV corresponding to Mn $2p_{3/2}$ and Mn $2p_{1/2,}$ respectively. The Mn $2p_{3/2}$ peak is further resolved into two peaks at 639.8 eV and 641.1 eV, corresponding to Mn^{2+} and Mn^{3+} respectively (Fig. 1e). However, no resolved peak for Mn(IV) ion could be found. By comparing their intensities, the surface ratio of Mn^{2+} to Mn^{3+} is found to be 1:1.7, which is comparable to the ratio of the proposed mixed-valence compound in the above elemental analysis. It further confirms the co-existence of divalent and trivalent manganese in the as-synthesized MnGly catalyst. It is reported that the divalent high-spin manganese complex adopts a d^5 electronic configuration. They do not exhibit a specific stereochemical preference due to a slight change of crystal field stabilization energy, and thus both tetrahedral and octahedral coordination geometry can be exchanged depending on the structural demand of the coordinated ligands [27]. Interestingly, there is a direct correlation between the catalytic biodiesel synthesis and the multivalent state of Mn in the MnGly catalyst as the Mn^{2+} center could be coordinated to neutral alcohols and neutral carbonyls present in the reaction mixture during the catalysis.

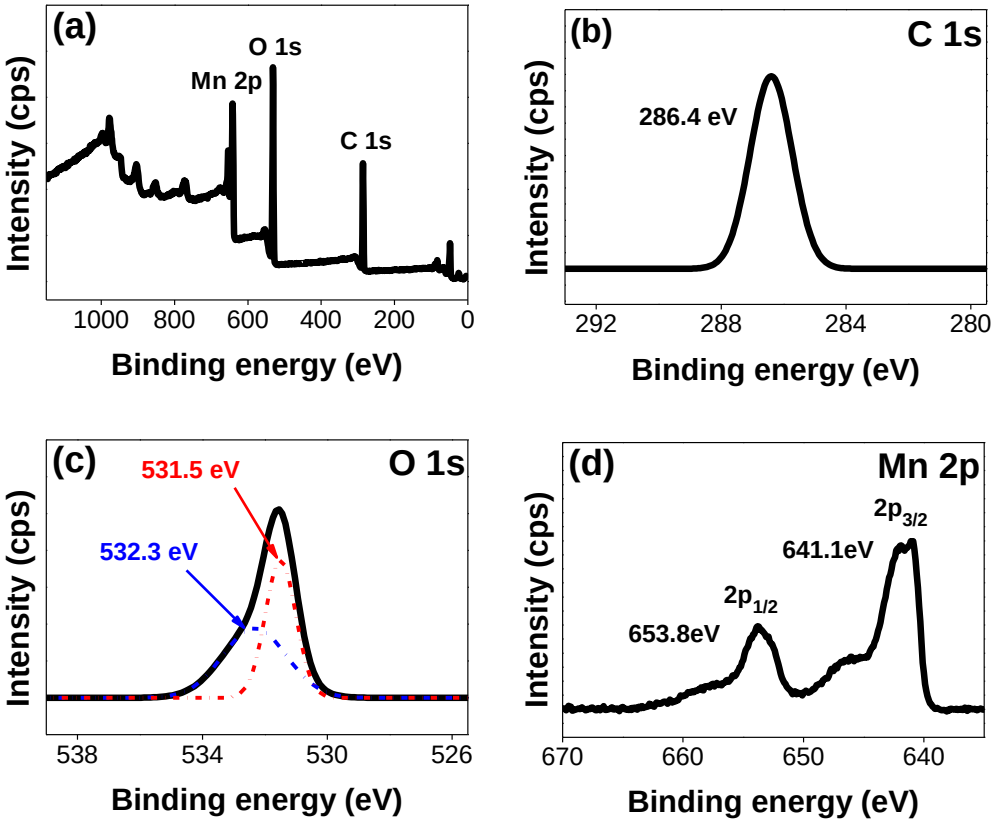

264

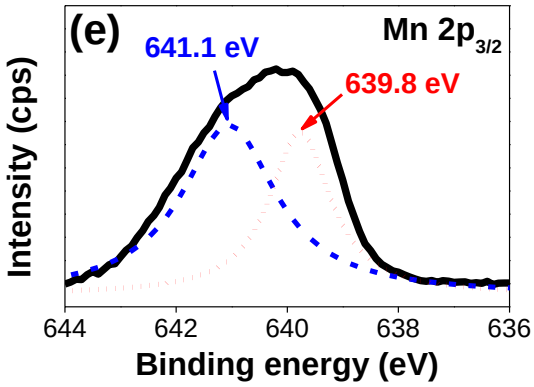

265

266 **Fig. 2.** (**a**) Full core XPS spectrum of MnGly nano-plate catalyst and the survey XPS spectra of (**b**) C
267 1s, (**c**) O 1s (**d**) Mn 2p, and (**e**) curve fitting for Mn $2p_{3/2}$.

268 *3.2. Reaction kinetics and determination of activation energy (E_a)*

269 The MnGly catalyzed simultaneous esterification and transesterification reaction for biodiesel
270 synthesis is assumed to consist of one reversible step of esterification of FFA and three consecutive
271 reversible steps of transesterification of triglyceride. However, as the rate of esterification differs from
272 the rate of transesterification, only the overall rate of simultaneous esterification and transesterification

can be examined based on biodiesel yield. The reaction temperature was found to be the most significant factor in affecting the catalytic yield of biodiesel, as mentioned from the above optimization analyses. In other words, the reaction temperature is the critical factor influencing the reaction rate.

To simplify the kinetic model based on the literature review, the overall reaction order of manganese glycerolate catalyzed transesterification could depend on the concentration of triglyceride and methanol. (1) The kinetic study was assumed as irreversible transesterification based on the date collection at the initial transesterification rate. (2) The excess methanol was used as the methanol to oil molar ratio of 40 to 1 which is larger than the theoretical value for transesterification, then the methanol concentration was assumed as a constant [28].

The kinetic study was performed with a ratio of feedstock sample-to-methanol (1:40), in which methanol should be an excess reactant and triglyceride was a limiting reactant. This kinetic study can also determine the order of reaction concerning triglyceride and methanol for the MnGly catalyzed reaction by fitting the data into the three scenarios through the linear regression approach shown in Table S1 in Supplementary materials. The correlation coefficients (R^2) of the scenarios are summarized and compared in Table 3. The highest R^2 among these three selected scenarios was scenario 1, with R^2 of 0.9969. Therefore, the reaction kinetics for MnGly catalyzed biodiesel synthesis can be recognized as a zero-order, revealing that the reaction rate is independent of the initial concentration of reactants. Changing the concentration does not affect the overall reaction rate. It is proposed that the catalytic system probably relies on the catalyst surface. Furthermore, a classical model with the linear equations (Equations S4-S6) as shown in Table S2 in Supplementary material revealed that the calculated R^2 for zero-, first-, and second-order at 150 °C were 0.9969, 0.9822, and 0.9290 respectively. It also further confirmed that the MnGly catalyzed biodiesel synthesis is followed zero-order reaction kinetics.

Generally, it is mainly attributed to the availability of adsorption sites on the catalyst surface rather than the methanol concentration [29]. This kinetic study suggested that the mechanism of MnGly catalyzed biodiesel synthesis involves the coordination of methanol to the Mn^{2+} center. The XPS results imply the co-existence of divalent and trivalent of manganese in MnGly catalyst in which the high-spin d^5 Mn^{2+} exhibits no coordination preference with a flexible interchangeable coordination geometry between tetrahedral and octahedral. Furthermore, the BJH analysis revealed that the pore diameter of 2.94 nm is large enough to accommodate methanol moiety that possesses a diameter of 0.36 nm [30].

It facilitates the coordination of two equivalence of methanol to Mn^{2+} center during the first step of biodiesel synthesis, becoming an octahedral geometry.

Table 3

The correlation coefficients, R^2, of MnGly catalyzed biodiesel synthesis at 150 °C for all eight scenarios.

Scenario	Reaction order		Overall order	Correlation coefficient (R^2)
	Triglyceride α	Methanol β		
1	0	0	0	0.9969
2	1	0	1	0.9822
3	2	0	2	0.9072

From the reaction rate constant (k) at each temperature determined from the linear plots of the zero-order reaction model (scenario 1) as displayed in Fig.S2 and Table S3 in Supplementary materials, the activation energy (E_a) of the MnGly catalyzed biodiesel synthesis can be estimated according to Arrhenius plot (Equation 8) as depicted in Fig. 3 with a slope of -13561. The activation energy of this catalytic system is calculated to be 112.7 kJ mol^{-1} which implies that a surface-mediated three-phase catalytic reaction system is involved and mass transfer limit would be a dominant factor [31]. The activation energy is much higher than that of the homogeneous catalysis reported in the literature, with a range of 26.78 kJ mol^{-1} to 83.68 kJ mol^{-1} [32].

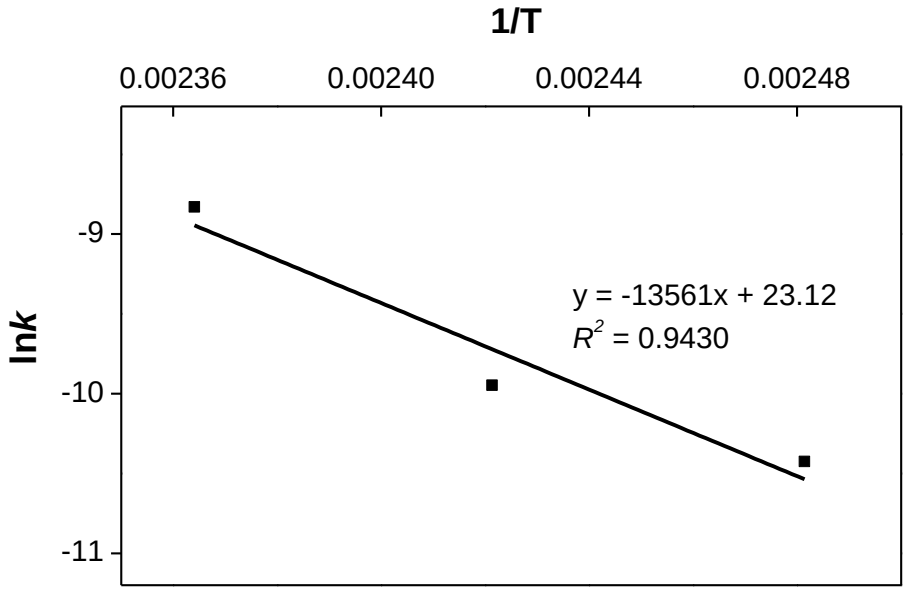

317

318 **Fig. 3.** The Arrhenius plot of ln*k* against 1/T for the MnGly catalyzed biodiesel synthesis.

319

320 *3.3. Proposed mechanism of MnGly catalyzed reaction*

321 The proposed mechanism for MnGly catalyzed biodiesel synthesis is depicted in Scheme 1. The
322 activation energy of MnGly catalyzed biodiesel synthesis suggests surface-mediated catalysis.
323 According to the result obtained in the kinetic study, the first step involves the coordination of two
324 methanol molecules to a high-spin d^5 Mn^{2+} center with an octahedral geometry, generating a methoxide
325 anion. The methoxide anion would then nucleophilic attack the carbonyl carbon of incoming fatty acid
326 or triglyceride molecule to yield FAME.

327

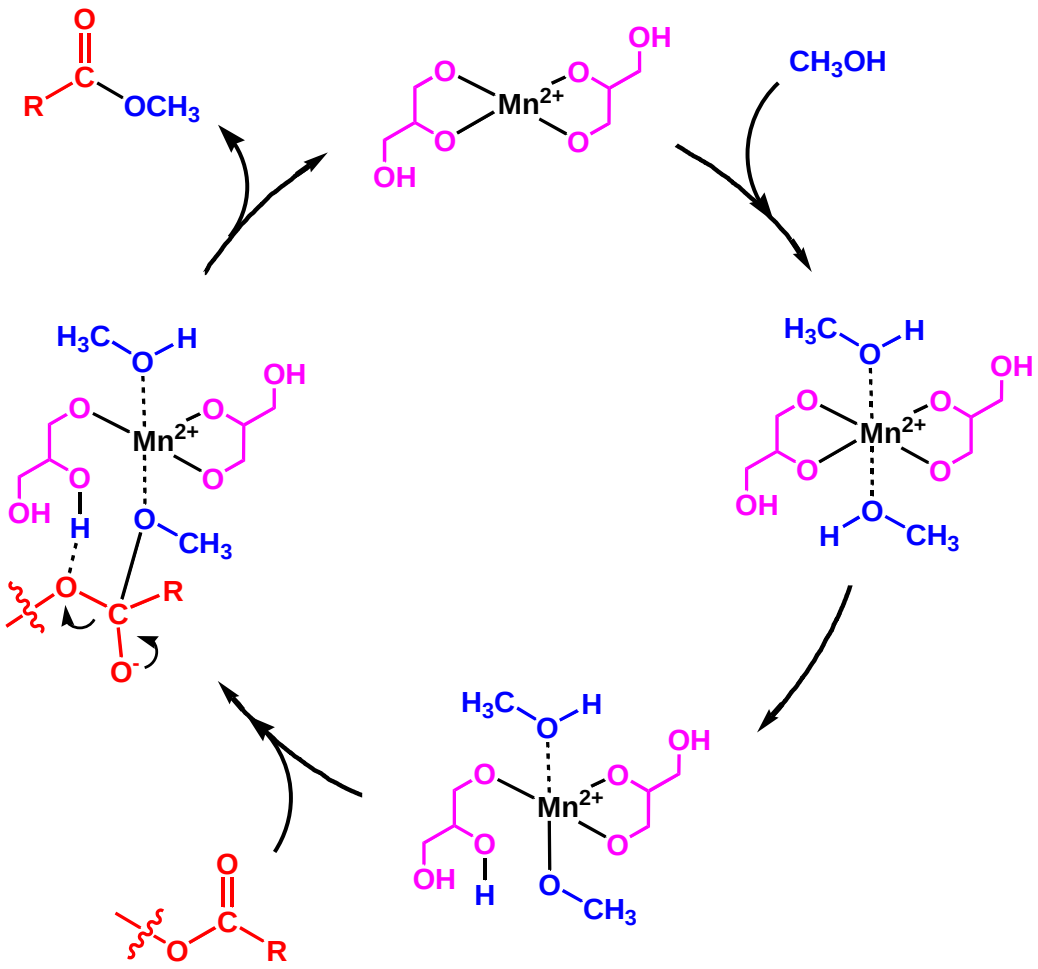

Scheme 1. Proposed mechanism for MnGly catalyzed reaction.

3.4. Catalytic optimization

An OA_{16} matrix was employed to assign all the factors and levels. Sixteen experimental runs of different combinations of factors and levels were conducted and each experimental run was triplicated to minimize random errors. Table 4 summarizes the orthogonal array matrix with the corresponding triplicated data of yield, S/N ratio, and standard deviation. The result of range analysis, including $\overline{S_{ji}}$ and R_j values are shown in Table 5. From the result of range analysis, the highest $\overline{S_{ji}}$ values are attained when the reaction temperature is 150 °C ($\overline{S_{A4}}$ = 37.5), feedstock-to-methanol molar ratio is 1:40 ($\overline{S_{B4}}$ = 30.7), the catalyst loading is 6 wt.% ($\overline{S_{C3}}$ = 30.2) and the oleic acid loading is 7.5 wt.% ($\overline{S_{D3}}$ = 30.9). Therefore, it can be concluded that the optimal reaction conditions are designated as $A_4B_4C_3D_3$. A confirmation experiment for MnGly catalyzed simultaneous esterification and transesterification was

then carried out. Based on the R_j values from range analysis, the reaction temperature is the most significant factor where the degree of significance of factors followed the order: reaction temperature (17.3) > oleic acid loading (4.9) > feedstock-to-methanol molar ratio (4.1) > catalyst loading (3.2). The largest range value of reaction temperature implies a significant effect on the yield for biodiesel synthesis upon a small change in temperature, whereas the small range value of catalyst loading denotes any changes in the catalyst loading caused the little effect on the yield.

Table 4

A summary of biodiesel yield in the optimization process.

Entry	Factor				Yield [a] (%)			Average Yield (%)	S/N ratio	Standard deviation
	A	B	C	D	y_1	y_2	y_3			
1	120	1:10	2	2.5	4.3	3.8	3.9	4.0	12.00	0.3
2	120	1:20	4	5	10.6	10.4	10.3	10.4	20.37	0.2
3	120	1:30	6	7.5	15.3	15.8	15.9	15.7	23.90	0.3
4	120	1:40	8	10	16.8	18.8	17.0	17.5	24.84	1.1
5	130	1:10	4	7.5	21.7	22.7	21.3	21.9	26.80	0.7
6	130	1:20	2	10	24.2	23.3	24.5	24.0	27.60	0.6
7	130	1:30	8	2.5	19.4	20.4	18.7	19.5	25.78	0.9
8	130	1:40	6	5	28.0	28.7	28.5	28.4	29.06	0.4
9	140	1:10	6	10	37.4	38.3	39.1	38.3	31.65	0.9
10	140	1:20	8	7.5	49.6	51.1	48.8	49.8	33.95	1.2
11	140	1:30	2	5	30.8	29.9	28.6	29.8	29.46	1.1
12	140	1:40	4	2.5	31.5	31.2	32.4	31.7	30.02	0.6
13	150	1:10	8	5	62.9	63.0	62.5	62.8	35.96	0.3
14	150	1:20	6	2.5	63.8	62.7	62.8	63.1	36.00	0.6
15	150	1:30	4	10	92.7	91.3	92.7	92.2	39.30	0.8
16	150	1:40	2	7.5	87.8	88.1	89.4	88.4	38.93	0.9

[a] Reaction conditions: reaction time (45 min).

Table 5

Result for range analysis.

	Reaction temperature A (°C)	Feedstock-to-methanol molar ratio B	Catalyst loading C (wt.%)	Oleic acid loading D (wt.%)
$\overline{S_1}$	20.3	26.6	27.0	26.0
$\overline{S_2}$	27.3	29.5	29.1	28.7
$\overline{S_3}$	31.3	29.6	30.2	30.9
$\overline{S_4}$	37.5	30.7	30.1	30.8
R_j	17.3	4.1	3.2	4.9

It can be observed that the $\overline{S_{Ai}}$ values increased significantly from 20.3 to 37.5 when the reaction temperature increased from 120 °C to 150 °C. This could be attributed to the inhibition of mass transfer in the reaction medium. As the use of solid MnGly catalyst creates a three-phase system of feedstock-methanol-catalyst, the reaction can only occur at the interface of the triple-phase and the rate of reaction is under mass transfer-controlled [21, 33]. Therefore, the increase in reaction temperature enhances the rate of diffusion and rate of reaction. It was found that the $\overline{S_{Bi}}$ values increased from 26.6 to 30.7 when the feedstock-to-methanol molar ratio changed from 1:10 to 1:40. As the transesterification process involves three consecutive reversible reactions in converting triglyceride into diglyceride, monoglyceride, and fatty acid methyl esters, a high feedstock-to-methanol molar ratio is desirable to shift the equilibrium to the product side [34, 35]. The result shows that increasing the amount of methanol to a ratio of 1:40 would further shift the equilibrium position from the reactant side to the product side. Besides, varying the catalyst loading from 2 wt.% to 6 wt.% increased the $\overline{S_{Ci}}$ values from 27.0 to the maximum point at 30.2 but slightly decreased when the catalyst loading was further increased to 8 wt.% (30.1). The initial increase could be ascribed to the enhanced availability of active sites on the catalyst surface [36, 37]. The slight reduction beyond the optimal point might be due to the mass transfer inefficiency caused by the presence of an excess catalyst. Finally, the $\overline{S_{Di}}$ values increased steadily from 26.0 when the oleic acid loading was 2.5 wt.% and achieved a maximum at 7.5

wt.% (30.9). The enhancement in biodiesel yield in the addition of more oleic acid suggests the occurrence of simultaneous esterification of FFA and transesterification of triglyceride in which the rate of esterification reaction is faster than that of transesterification reaction. Warabi *et al.* [38] proposed that the solubility of unsaturated fatty acid in methanol is higher than that of triglyceride, so the mass transfer efficiency of the reaction system is enhanced in the presence of FFA. Moreover, it is believed that the activation barrier of one-step esterification of FFA is lower than that of three-step transesterification of triglyceride in biodiesel synthesis. Thus, the rate of esterification would proceed faster than that of transesterification and the overall rate of simultaneous esterification and transesterification reaction would be enhanced with the presence of more FFA.

The results of ANOVA are summarized in Table 6. At the 90% confidence level, the critical value $F_{0.1}(3,3)$ is 5.39. By the comparison of F values with the critical value, it shows that $F_A > F_\alpha$; $F_B > F_\alpha$; $F_C > F_\alpha$ and $F_D > F_\alpha$. Therefore, all four factors are qualitatively identified to be prominent factors in this catalytic system by the F-test. Based on the percentage contribution, the relative power of the four factors followed the order: reaction temperature (82.84%) > oleic acid loading (8.61%) > feedstock-to-methanol molar ratio (4.87%) > catalyst loading (3.48%). This trend is consistent with the result obtained from Taguchi analysis. It should be noted that the percentage contribution of experimental error is only as low as 0.2%. Hence, it is concluded that no other important factors had been omitted in this optimization process.

Table 6

Results for analysis of variance (ANOVA).

Factor	**SS_j**	**df_j**	**V_j**	**F_j**	**$F_{0.1}(3,3) = 5.39$**	**P_j (%)**
A	628.33	3	209.44	410.97	>	82.84
B	36.96	3	12.32	24.18	>	4.87
C	26.36	3	8.79	17.24	>	3.48
D	65.33	3	21.78	42.73	>	8.61
Error	1.53	3	0.51	–	–	0.20
Sum	758.52	15	–	–	–	100.00

3.5. Exploration on MnGly catalyzed biodiesel and bio-lubricants synthesis using different alcohols

This MnGly catalytic system was also further investigated in the application of bio-lubricant preparation. Bio-lubricants have been reported that extensively utilized in auto-mobile sectors and industries for lubricating working machines and materials. It can be produced using different feedstock (edible oil, non-edible oil, waste cooking oil, etc.) with higher alcohols (*n*-hexanol, *n*-heptanol, etc.) to form fatty acid alkyl (hexyl and heptyl) esters through simultaneous esterification and transesterification [39]. To investigate the effect of the types of alcohol on MnGly catalyzed simultaneous esterification and transesterification, different types of alcohol were applied under the optimized conditions.

The results as indicated in Table 7 displayed a decreasing trend in the catalytic activity when the chain length of alcohol increases but levelled off from 1-butanol onwards after 1.5 hours. It indicates that methanolysis proceeds at a faster rate than all other alcohols. This could be attributed to the higher reactivity of methoxide anion than other alkoxide anions since an increase in the carbon chain length of alkoxide anion would lead to a destabilization of alkoxide anions through the positive inductive effect that causes a decrease in their nucleophilicity in the generation of fatty acid alkyl ester [40]. It should be noted that 1-butanol, 1-pentanol, 1-hexanol and 1-heptanol are completely miscible with oil owing to their lower polarity than methanol, ethanol and 1-propanol. Thus, those long-chain alcohols would proceed in the monophasic state, which is free from mass transfer resistance. Miscibility might be the dominating factor over nucleophilicity of the corresponding alkoxide anion for long-chain alcohols in biodiesel synthesis. Therefore, the rate of reaction from 1-butanol to 1-heptanol remained almost the same. All alcohols achieved over 99% yield in a 3-hour time.

Table 7

Effect of alcohols on MnGly catalyzed biodiesel and bio-lubricants synthesis.

Entry	Alcohol	Chemical formula	Yield [a] (%)	
			1.5 h	3 h
1	Methanol	CH_3OH	99.1	–
2	Ethanol	C_2H_5OH	95.3	99.2
3	1-propanol	C_3H_7OH	72.6	99.7
4	1-butanol	C_4H_9OH	70.6	99.1
5	1-pentanol	$C_5H_{11}OH$	70.4	99.0
6	1-hexanol	$C_6H_{13}OH$	70.4	99.8
7	1-heptanol	$C_7H_{15}OH$	70.2	99.6

[a] Reaction conditions: reaction temperature (150 °C), feedstock-to-methanol (1:40), catalyst loading (6 wt.%), and oleic acid loading (7.5 wt.%).

3.6. Study of microwave-assisted MnGly catalyzed biodiesel synthesis

The conventional heating, the heat is mainly transferred by conduction and convection. Moreover, some heat energy may localize in a particular site as heat transfer depends on the material properties such as specific heat capacity, density and thermal conductivity. Microwave irradiation, an energy-efficient heating technique, has recently proved to minimize the mass transfer limit with the instant interaction of a reaction mixture [41].

The microwave-assisted MnGly catalyzed biodiesel synthesis was then investigated under the optimized reaction conditions. The results from Table 8 indicated that the time required to complete the biodiesel synthesis with 97.6% yield is shortened to only 1 hour at 150 °C, which is faster than under conventional heating requiring 1.5 h, demonstrating that microwave irradiation is a more energy-efficient heating technique over conventional heating. It is noticed that once the reaction temperature is raised to 160 °C, the time required can be significantly reduced to half an hour.

Table 8

Time required for microwave-assisted MnGly catalyzed biodiesel synthesis at different temperatures.

Entry	Reaction Temperature (°C)	Reaction Time (h)	Yield [a] (%)
1	160	0.5	97.3
2	150	1	97.6
3	140	2	95.6
4	130	4	95.3
5	120	7	95.0

[a] Reaction conditions: feedstock-to-methanol (1:40), catalyst loading (6 wt.%) and oleic acid loading (7.5 wt.%), and microwave power (200 W).

4. Conclusion

MnGly catalyst was further investigated using different physical characterizations. The elemental analysis confirms that the chemical formula of MnGly catalyst is $C_{12}H_{24}O_{12}Mn_3$ in which the ratio of Mn-to-Gly is found to be 3:4. It is likely to exist as a mixed-valence compound in an Mn^{2+} to Mn^{3+} ratio of 1:2. The XPS analysis also revealed the co-existence of divalent and trivalent manganese in MnGly catalyst with Mn^{2+} to Mn^{3+} ratio of 1:1.7, which is comparable to the result in elemental analysis. The average pore diameter on the catalyst surface is found to be 2.94 nm which is large enough to accommodate methanol. Two equivalence of methanol would coordinate to high-spin Mn^{2+} center to form octahedral geometry. The activation energy is calculated as 112.7 kJ $mol^{-1,}$ which indicates surface-mediated heterogeneous catalysis. The reaction conditions were optimized through Taguchi analysis with the OA_{16} matrix. According to range analysis, the optimized conditions were designated as reaction temperature (150 °C), feedstock-to-methanol molar ratio (1:40), catalyst loading (6 wt.%), and oleic acid loading (7.5 wt.%). Based on the results obtained from range analysis and ANOVA, the reaction temperature is found to be the most significant factor with an 82.84% contribution for biodiesel synthesis. This catalytic system can be applied in bio-lubricants production using higher alcohols with over 99% yield in 3 hours. It is also proved that microwave irradiation is a more energy-efficient heating

technique as the reaction time is shortened with the comparable biodiesel yield (97.6%) compared to conventional heating.

CRediT authorship contribution statement

Pak-Chung Lau: Methodology, Investigation, Writing - original draft, Visualization. **Tsz-Lung Kwong:** Conceptualization, Methodology, Formal analysis, Resources, Writing - review & editing, Visualization, Supervision, Project administration. **Ka-Fu Yung:** Conceptualization, Resources, Writing - review & editing, Supervision, Funding acquisition.

Declaration of competing interest

The authors declare that they have no known competing financial interests or personal relations that could have appeared to influence the work reported in this paper.

Acknowledgements

The authors would like to acknowledge the financial support from The Hong Kong Polytechnic University with grant numbers PolyU 153053/17P and PolyU P0032339. The authors are also very grateful to thank the University Research Facility in Chemical and Environmental Analysis (UCEA) of The Hong Kong Polytechnic University for supporting the analytical instruments used in this research study.

Supplementary materials

Supplementary information to this article can be found at http://.

References

[1] S.Y. Chua, C.M.H. Goh, Y.H. Tan, N.M. Mubarak, J. Kansedo, M. Khalid, R. Walvekar, E. Abdullah, Biodiesel synthesis using natural solid catalyst derived from biomass waste—A review, J. Ind. Eng. Chem. 81 (2020) 41-60.

[2] G. Joshi, J.K. Pandey, S. Rana, D.S. Rawat, Challenges and opportunities for the application of biofuel, Renew. Sustain. Energy Rev. 79 (2017) 850-866.

[3] G. Guan, N. Sakurai, K. Kusakabe, Synthesis of biodiesel from sunflower oil at room temperature in the presence of various cosolvents, Chem. Eng. J. 146(2) (2009) 302-306.

[4] J.F. Sierra-Cantor, C.A. Guerrero-Fajardo, Methods for improving the cold flow properties of biodiesel with high saturated fatty acids content: a review, Renew. Sustain. Energy Rev. 72 (2017) 774-790.

[5] L.-F. Man, T.-L. Kwong, W.-T. Wong, K.-F. Yung, Mesoporous Zn/MgO Hexagonal Nano-Plates as a Catalyst for Camelina Oil Biodiesel Synthesis, Nanomater. 11(10) (2021) 2690.

[6] B. Karmakar, G. Halder, Progress and future of biodiesel synthesis: advancements in oil extraction and conversion technologies, Energy Convers. Manag. 182 (2019) 307-339.

[7] M.K. Yesilyurt, C. Cesur, V. Aslan, Z. Yilbasi, The production of biodiesel from safflower (Carthamus tinctorius L.) oil as a potential feedstock and its usage in compression ignition engine: A comprehensive review, Renew. Sustain. Energy Rev. 119 (2020) 109574.

[8] D. Kour, K.L. Rana, N. Yadav, A.N. Yadav, A.A. Rastegari, C. Singh, P. Negi, K. Singh, A.K. Saxena, Technologies for biofuel production: current development, challenges, and future prospects, Prospects of renewable bioprocessing in future energy systems, Springer, Cham2019, pp. 1-50.

[9] B. Freedman, E. Pryde, T. Mounts, Variables affecting the yields of fatty esters from transesterified vegetable oils, J. Am. Oil Chem. Soc. 61(10) (1984) 1638-1643.

[10] I.B. Laskar, T. Deshmukhya, P. Bhanja, B. Paul, R. Gupta, S. Chatterjee, Transesterification of soybean oil at room temperature using biowaste as catalyst; an experimental investigation on the effect of co-solvent on biodiesel yield, Renew. Energy 162 (2020) 98-111.

[11] M.B. Navas, I.D. Lick, P.A. Bolla, M.L. Casella, J.F. Ruggera, Transesterification of soybean and castor oil with methanol and butanol using heterogeneous basic catalysts to obtain biodiesel, Chem. Eng. Sci. 187 (2018) 444-454.

[12] I. Ambat, V. Srivastava, M. Sillanpää, Recent advancement in biodiesel production methodologies using various feedstock: A review, Renew. Sustain. Energy Rev. 90 (2018) 356-369.

[13] F.d.S. Lisboa, J.E.F.d. Gardolinski, C.S. Cordeiro, F. Wypych, Layered metal laurates as active catalysts in the methyl/ethyl esterification reactions of lauric acid, J. Braz. Chem. Soc. 23(1) (2012) 39-45.

[14] M.S. Alvarez Serafini, G.M. Tonetto, Synthesis of fatty acid methyl esters from pomace oil catalyzed by zinc stearate: a kinetic study of the transesterification and esterification reactions, Catal. 9(12) (2019) 978.

[15] D.M. Reinoso, D.E. Damiani, G.M. Tonetto, Zinc glycerolate as a novel heterogeneous catalyst for the synthesis of fatty acid methyl esters, Appl. Catal. B: Environ. 144(0) (2014) 308-316.

[16] T.-L. Kwong, K.-F. Yung, One-step production of biodiesel through simultaneous esterification and transesterification from highly acidic unrefined feedstock over efficient and recyclable ZnO nanostar catalyst, Renew. Energy 90 (2016) 450-457.

[17] P.-C. Lau, T.-L. Kwong, K.-F. Yung, Effective heterogeneous transition metal glycerolates catalysts for one-step biodiesel production from low grade non-refined Jatropha oil and crude aqueous bioethanol, Sci. Rep. 6(1) (2016) 23822.

[18] S.Z. Hassan, M. Vinjamur, Parametric effects on kinetics of esterification for biodiesel production: A Taguchi approach, Chem. Eng. Sci. 110 (2014) 94-104.

[19] X. Wu, D.Y.C. Leung, Optimization of biodiesel production from camelina oil using orthogonal experiment, Appl. Energy 88(11) (2011) 3615-3624.

[20] C. Chuanwen, S. Feng, L. Yuguo, W. Shuyun, Orthogonal analysis for perovskite structure microwave dielectric ceramic thin films fabricated by the RF magnetron-sputtering method, J. Mater. Sci.: Mater.in Electron. 21(4) (2010) 349-354.

[21] T.-L. Kwong, K.-F. Yung, Heterogeneous alkaline earth metal–transition metal bimetallic catalysts for synthesis of biodiesel from low grade unrefined feedstock, RSC Adv. 5(102) (2015) 83748-83756.

[22] L. Meher, D.V. Sagar, S. Naik, Technical aspects of biodiesel production by transesterification—a review, Renew. Sustain. Energy Rev. 10(3) (2006) 248-268.

[23] A.K. Singh, S.D. Fernando, Reaction kinetics of soybean oil transesterification using heterogeneous metal oxide catalysts, Chem. Eng. & Technol.: Ind. Chem.-Plant Equip.-Process Eng.-Biotechnol. 30(12) (2007) 1716-1720.

[24] L.A. Román-Ramírez, P. McKeown, M.D. Jones, J. Wood, Kinetics of methyl lactate formation from the transesterification of polylactic acid catalyzed by Zn (II) complexes, ACS Omega 5(10) (2020) 5556-5564.

[25] F. Ambroz, T.J. Macdonald, V. Martis, I.P. Parkin, Evaluation of the BET Theory for the Characterization of Meso and Microporous MOFs, Small Methods 2(11) (2018) 1800173.

[26] J. Yin, K. Song, Y. Lu, G. Zhao, Y. Yin, Comparison of changes in micropores and mesopores in the wood cell walls of sapwood and heartwood, Wood Sci. Technol. 49(5) (2015) 987-1001.

[27] I. Syiemlieh, A. Kumar, S.D. Kurbah, A.K. De, R.A. Lal, Low-spin manganese (II) and high-spin manganese (III) complexes derived from disalicylaldehyde oxaloyldihydrazone: Synthesis, spectral characterization and electrochemical studies, J. Mol. Struct. 1151 (2018) 343-352.

[28] A. Kapil, K. Wilson, A.F. Lee, J. Sadhukhan, Kinetic modeling studies of heterogeneously catalyzed biodiesel synthesis reactions, Ind. Eng. Chem. Res. 50(9) (2011) 4818-4830.

[29] Y. Liu, New insights into pseudo-second-order kinetic equation for adsorption, Colloids and Surf. A: Physicochem. and Eng. Asp. 320(1-3) (2008) 275-278.

[30] H. Hu, J. Zhu, F. Yang, Z. Chen, M. Deng, L. Weng, Y. Ling, Y. Zhou, A robust etb-type metal–organic framework showing polarity-exclusive adsorption of acetone over methanol for their azeotropic mixture, Chem. Commun. 55(46) (2019) 6495-6498.

552 [31] M.D. Kostić, A. Bazargan, O.S. Stamenković, V.B. Veljković, G. McKay, Optimization and kinetics
553 of sunflower oil methanolysis catalyzed by calcium oxide-based catalyst derived from palm kernel shell
554 biochar, Fuel 163 (2016) 304-313.

555 [32] X. Liu, X. Piao, Y. Wang, S. Zhu, Calcium ethoxide as a solid base catalyst for the transesterification
556 of soybean oil to biodiesel, Energy & Fuels 22(2) (2008) 1313-1317.

557 [33] S. Gryglewicz, Rapeseed oil methyl esters preparation using heterogeneous catalysts, Bioresour.
558 Technol. 70(3) (1999) 249-253.

559 [34] V.K. Booramurthy, R. Kasimani, D. Subramanian, S. Pandian, Production of biodiesel from tannery
560 waste using a stable and recyclable nano-catalyst: an optimization and kinetic study, Fuel 260 (2020)
561 116373.

562 [35] M. Kavitha, S. Murugavelh, Optimization and transesterification of sterculia oil: Assessment of
563 engine performance, emission and combustion analysis, J. Clean. Prod. 234 (2019) 1192-1209.

564 [36] Y. Zhang, W.-T. Wong, K.-F. Yung, Biodiesel production via esterification of oleic acid catalyzed
565 by chlorosulfonic acid modified zirconia, Appl. Energy 116(0) (2014) 191-198.

566 [37] O. Khan, M.E. Khan, A.K. Yadav, D. Sharma, The ultrasonic-assisted optimization of biodiesel
567 production from eucalyptus oil, Energy Sour, Part A: Recovery, Utilization, and Environ. Eff. 39(13)
568 (2017) 1323-1331.

569 [38] Y. Warabi, D. Kusdiana, S. Saka, Reactivity of triglycerides and fatty acids of rapeseed oil in
570 supercritical alcohols, Bioresour. Technol. 91(3) (2004) 283-287.

571 [39] E. Kleinaitė, V. Jaška, B. Tvaska, I. Matijošytė, A cleaner approach for biolubricant production using
572 biodiesel as a starting material, J. Clean. Prod. 75 (2014) 40-44.

573 [40] B.R. Moser, Biodiesel production, properties, and feedstocks, In Vitro Cell. & Dev. Biol.-Plant 45(3)
574 (2009) 229-266.

575 [41] I. Choedkiatsakul, K. Ngaosuwan, S. Assabumrungrat, S. Tabasso, G. Cravotto, Integrated flow
576 reactor that combines high-shear mixing and microwave irradiation for biodiesel production, Biomass
577 and Bioenergy 77 (2015) 186-191.